ETHANOL SENSING PROPERTY OF α-Fe_2O_3 NANORODS/ZnO NANOPARTICLES COMPOSITES

Lương Hữu Phước, Nguyễn Đắc Diện*, Đỗ Đức Thọ, Vũ Xuân Hiền, Đặng Đức Vượng
School of Engineering Physics, Hanoi University of Science and Technology
No.1 Dai Co Viet road, Hanoi city, Vietnam
Email address: nddien1980@yahoo.ca ; Tel.: +84975528087

Abstract

α-Fe_2O_3 was synthesized via hydrothermal treatment at 140 °C for 24 h using $Fe(NO_3)_3.9H_2O$ and Na_2SO_4 as the raw materials. ZnO was prepared by soft chemical process using $Zn(NO_3)_2$ and $(NH_4)_2CO_3$ as precursors. Field emission scanning electron microscopy (FESEM) images showed that the as-prepared α-Fe_2O_3 had rod-like morphology with the diameter of 30-50 nm and 200-300 nm in length, and the shape of ZnO was nanoparticle with the size of 20-30 nm. The α-Fe_2O_3/ZnO composites were obtained by grinding α-Fe_2O_3 NRs powder with ZnO NPs powder in various weight ratios (Fe_2O_3/ZnO = 80/20, 70/30, 60/40, 50/50, 40/60, 30/70, 20/80). The gas sensing properties of composite films were tested with ethanol, LPG and ammonia, where the concentrations ranged from 250 to 2000 ppm and temperatures in the range of 300-400 °C. α-Fe_2O_3/ZnO composite corresponding to 60 wt.% of α-Fe_2O_3 exhibited superior sensing characteristic towards ethanol vapor comparing to other samples. Its sensor response is 48, which is 3 times higher than that of pure α-Fe_2O_3 and 5 times higher than that of pure ZnO towards 2000 ppm C_2H_5OH at an operating temperature of 350 °C. Moreover, the response rate was very quick with response time within 30 s. Finally, the mechanism for the improvement in the gas sensing property was discussed.

Keywords: ethanol sensor, α-Fe_2O_3/ZnO composite, hydrothermal treatment.

1. Introduction

Metal oxide semiconductor gas sensors are extensively applied in detection of toxic gases (e.g., NH_3, H_2S, NO, etc.) and volatile organic compounds (e.g., C_2H_5OH, CH_3COCH_3, LPG, etc.) due to their great sensitivity and good selectivity as well as short response time. It is known that, the gas-sensing properties are strongly depended on the morphology [1], size [2, 3], porosity [4], surface properties [5] and composition [6]. Many efforts have focused on the modification of nanostructures by altering the amount and distribution of the constituents to improve the sensor 3S (sensitivity, selectivity and stability). Composite material is one effective solution for this problem.

α-Fe_2O_3 is an n-type semiconductor with a narrow band gap (E_g=2.2 eV) and its electrical conductivity is high sensitive to gaseous environments which has been used as a ethanol sensor [7]. In the past several years, coupled semiconductors formed by α-Fe_2O_3 and other metal oxides such as SnO_2, ZnO, TiO_2, CuO have been reported. Wei-Wei Wang prepared SnO_2/α-Fe_2O_3 hierarchical nanostructure through hydrothermal treatment [8]. Limei Huang and Huiqing Fan have synthesized ZnO/α-Fe_2O_3 hierarchical nanostructures via a facile solid state reaction route of zinc acetate, α-Fe_2O_3 and NaOH to enhance gas-sensing property to ethanol vapor [9]. D.R. Patil and L.A. Patil obtained Fe_2O_3 doped ZnO thick film which could response to NH_3 selectively in the presence of other hazardous and polluting gases such as LPG, CO_2, C_2H_5OH, etc. [10]. Monica Sorescu *et al*. synthesized the nanoparticle system α-Fe_2O_3/SnO_2 under hydrothermal conditions as 200 °C and 4 h [11]. α-Fe_2O_3 NRs/SnO_2 NRs composites prepared through hydrothermal treatment method exhibited higher response to

LPG at 370 °C compared with bare α-Fe_2O_3 NRs [12]. Gas sensors based on the Fe_2O_3-ZnO (with Fe:Zn=2%) nanoparticles composites prepared by a sol-gel method exhibited fairly excellent sensitivity and selectivity to NH_3 at room temperature, the response and recovery time of the sensor were both less than 20 s [13]. Fe_2O_3/TiO_2 nanocomposites were prepared using pulsed laser gas phase evaporation [14]. CuO/Fe_2O_3 composite was applied to oxidation catalyst [15].

In this contribution, we prepared α-Fe_2O_3/ZnO composites by blending α-Fe_2O_3 NRs powder and ZnO NPs powder which had been synthesized separately by hydrothermal treatment and studied their ethanol sensing properties. The experimental results exhibited much higher sensitivity than those of pristine α-Fe_2O_3 or ZnO.

2. Experimental

α-Fe_2O_3 NRs were synthesized by hydrothermal treatment using iron (III) nitrate nanohydrate $Fe(NO_3)_3.9H_2O$ and sodium sulfate Na_2SO_4 as precursors. The preparation basically involved three steps. First, 0.075 M $Fe(NO_3)_3$ solution and 0.075 M Na_2SO_4 solution were mixed together with volume ratio of 1:1 to form a homogeneous solution under magnetic stirring for 30 min. Second, the mixed solution was subjected to hydrothermal treatment at 140 °C for 24 h. Third, after cooling to ambient temperature, the collected reddish-brown solid was rinsed with distilled water and absolute ethanol several times and finally dried at 80 °C overnight to obtain the nanorods.

For preparing ZnO nanoparticles, zinc nitrate hexahydrate $Zn(NO_3)_2.6H_2O$ and ammonium carbonate $(NH_4)_2CO_3$ were used as precursors. In a typical synthesis, 100 ml $Zn(NO_3)_2$ solution (0.5 M) was gradually dropped to 150 ml $(NH_4)_2CO_3$ solution (0.5 M) during stirring in succession at 40 °C for 1 h. After that, the mixed solution was washed with distilled water and absolute ethanol several times and dried at 80 °C for 24 h in air. The obtained product was white-yellow powder.

The obtained α-Fe_2O_3 powder and ZnO powder were dispersed into ethanol and mixed together in the required proportions (α-Fe_2O_3: ZnO = 80:20, 70:30, 60:40, 50:50, 40:60, 30:70, 20:80 in weight) to form α-Fe_2O_3/ZnO composite materials.

The pure α-Fe_2O_3 powder, pure ZnO powder and α-Fe_2O_3/ZnO composites were characterized by X-ray diffraction (XRD, Bruker D8 Advance X-ray diffraction, using Cu-K_α radiation with a wavelength of 1.5406 Å over a scanning angle 2θ from 20° to 70°), field emission scanning electron microscopy (FESEM, Hitachi S4800) and energy dispersive X-ray spectroscopy (EDS, OXFORD JEOL 5410 LV).

The powders were grinded with ethanol and PEG (polyethylene glycol) in an agate mortar to form sticky slurry. Then, the slurry was coated onto Si/SiO_2 substrate attaching an interdigitated platinum electrode with finger width of 20 μm and gap size of 20 μm. After drying at 80 °C for 24 h, the sample was heated to 600 °C for 2 h in air. The gas sensing properties of these films were tested to C_2H_5OH, NH_3, LPG at operating temperature range of 300-400 °C and concentrations ranging from 250 to 2000 ppm. The sensors were tested by a static gas testing system. The sensor response is defined as $S=R_a/R_g$, where R_a and R_g are the resistance of the sensor in air and in target gas, respectively. The response time is defined as the time required reach 90% of the final equilibrium value and the recovery time is taken as the time necessary for the sensor to attain a resistance 10% below the original value in air.

3. Results and discussion

Fig.1 shows SEM images of the as-prepared samples which illustrated the morphology of the α-Fe_2O_3 NRs (Fig.1a), ZnO NPs (Fig.1b) and α-Fe_2O_3/ZnO nanocomposite (Fig.1c,d). The α-Fe_2O_3 powder contained nanorods with about 30-50 nm in diameter and 200-300 nm in length. The ZnO powder consists of relatively uniform nanoparticles with average size of 20-30 nm. Fig.1 (c,d) shows the low-magnification and high-magnification SEM images of α-Fe_2O_3/ZnO nanocomposite with weight ratio of 2/3. ZnO NPs are branched onto the surface of α-Fe_2O_3 NRs with commensurate dispersion. The dimensions of ZnO NPs and α-Fe_2O_3 NRs in the composite sample are almost the same as their dimensions in precursor samples. It indicates that α-Fe_2O_3/ZnO nanostructures are formed by many nanorods and the ZnO NPs play an important role in controlling the morphology. The nanorods are organized to form the regular three-dimensional nanostructures and ZnO NPs sprinkled well on the α-Fe_2O_3 NRs. When increasing ZnO content, an overdose of ZnO aggregated to form some irregular bulks which could destroy the rod-like morphology.

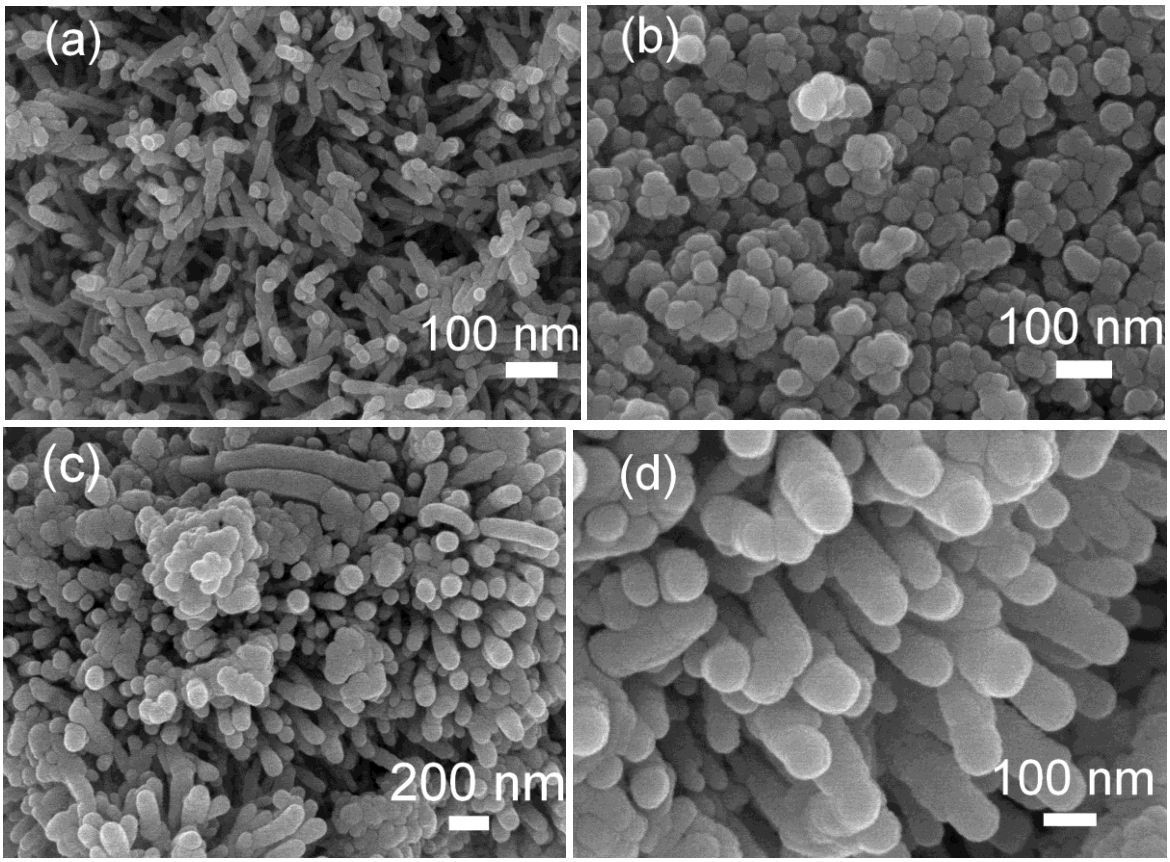

Figure 1. SEM images of α-Fe_2O_3 NRs (a), ZnO NPs (b), α-Fe_2O_3/ZnO composite with different magnifications of 35,000 (c) and 100,000 (d).

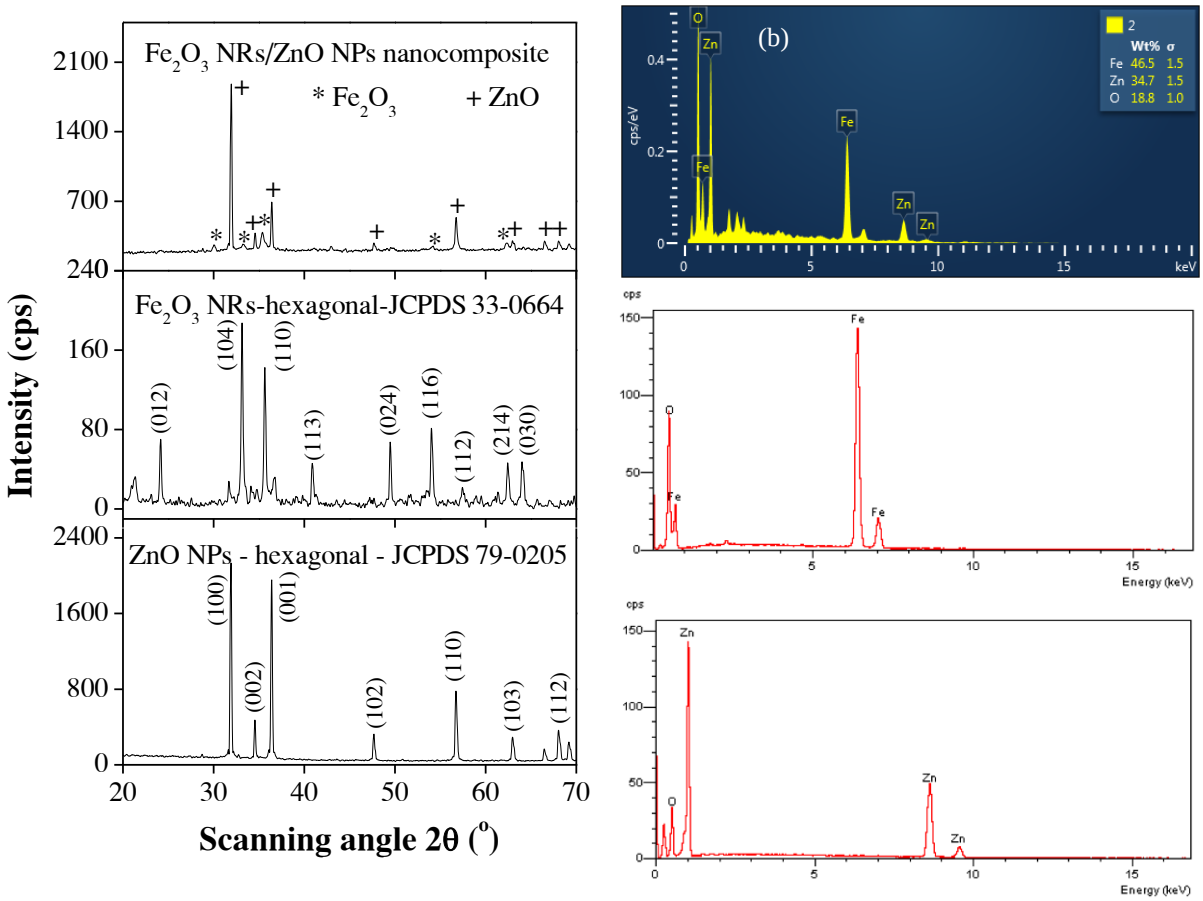

Figure 2. XRD pattern (a) and EDS pattern (b) of α-Fe_2O_3/ZnO composite.

Fig.2a shows the X-ray diffraction (XRD) patterns of blank ZnO, Fe_2O_3 and α-Fe_2O_3/ZnO composite. Crystal structure of ZnO NPs is hexagonal wurtzite with lattice constants of a=b=0.3242 nm, c=0.5188 nm, α=β=90°, γ=120°, space group P6/3mc in accordance with values in the standard card (JCPDS card No. 79-0205). Crystal structure of α-Fe_2O_3 NRs is hexagonal with lattice constants of a=b=0.5038 nm, c=1.3772 nm, α=β=90°, γ=120°, the space group R3c (JCPDS card No. 33-0664). It is note-worthy that the characteristic peaks of Fe_2O_3 can hardly be identified from the pattern of the composite. (104) reflection peak of Fe_2O_3 overlaps the peak of ZnO (100) reflection in the composite diffraction pattern. Additionally, the other peaks of Fe_2O_3 due to (012), (113), (024) at scanning angles of 24°, 41°, 49° respectively, where no peak can be attributed to ZnO, are also absent in the composite diffraction pattern. This observation can be assigned that the Fe_2O_3 nanorods are well embedded in the ZnO matrix.

The formation of α-Fe_2O_3/ZnO composite is confirmed from the EDS pattern. Result from EDS analysis of α-Fe_2O_3 NRs/ZnO NPs composite sample with the weight ratio of Fe_2O_3/ZnO=60/40 (Fig.2b) reveals that the products are formed by Zn, Fe and O elements. Semiquantitative estimation of the weight concentration (wt.%) exhibited that the composition results were almost consistent with the desired weight ratios of α-Fe_2O_3 and ZnO.

The adsorption, diffusion, and surface reaction rates between the target gas and the gas sensing layer can be influenced by the operating temperature, which will further affect the

sensor response. Therefore, we first investigate the optimum operating temperature for the sensors by sensing 2000 ppm C_2H_5OH from 300 to 400 °C. Gas sensitivity, as a function of the operating temperature, is shown in Fig.3a.

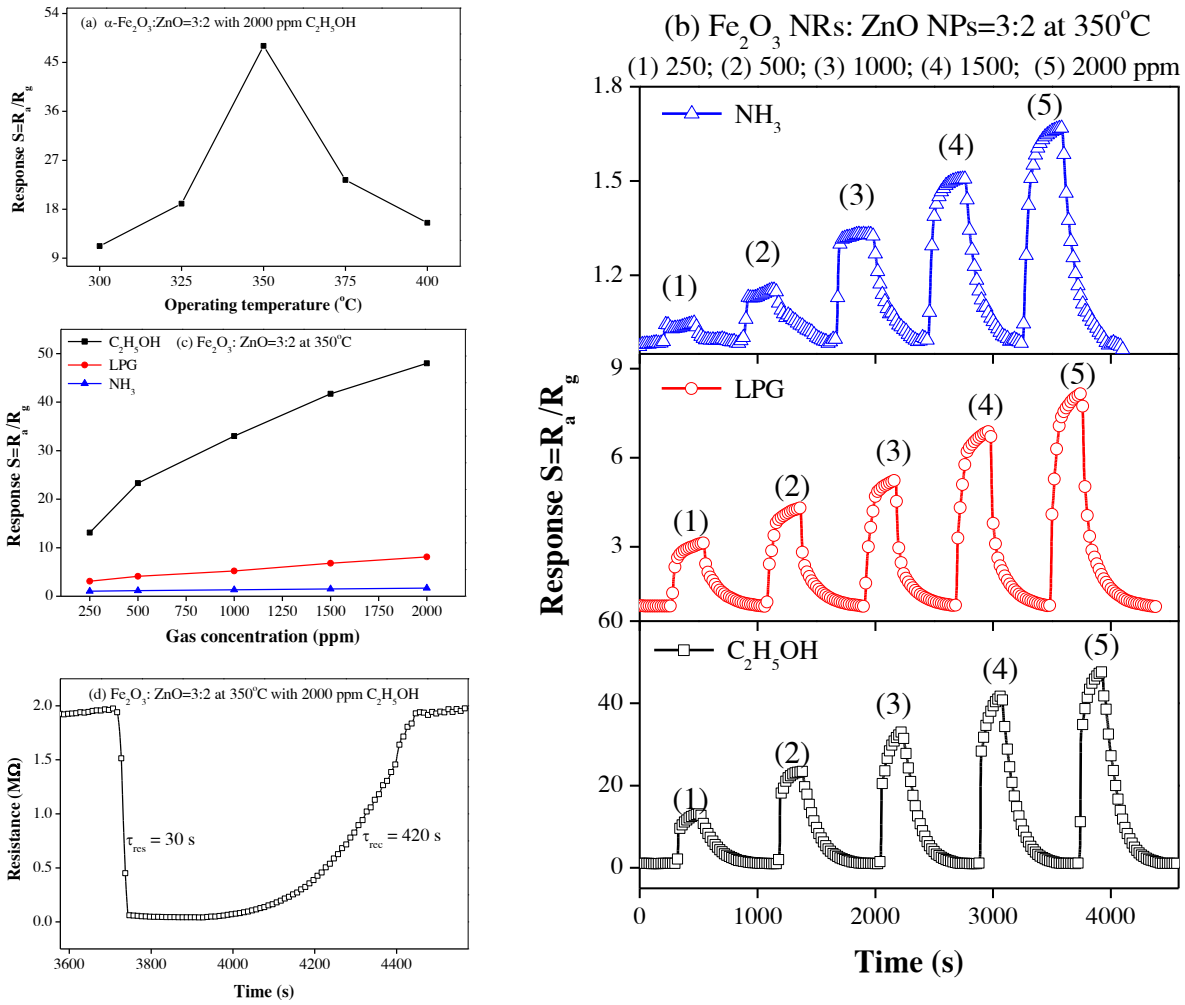

Figure 3. The gas-sensing properties of the sensor based α-Fe_2O_3/ZnO composite with weight ratio of 60/40 or 3/2.

The sensitivity of the sensors increases with the operating temperature increasing from 300 °C to 350 °C and then decrease as the operating temperature increases further. The reason is that in low operating temperature region (300 °C-350 °C), reaction rate increases with the increase of temperature, leading the increase of response; however, when the operating temperature is too high (above 350 °C), the desorption process becomes dominant and the diffusion depth becomes lower, which results in lower sensitivity. The optimum operating temperature to C_2H_5OH is about 350 °C and the maximum response reaches 48. Fig.3b shows the transient response curve of the sensor based on α-Fe_2O_3/ZnO composite with weight ratio of 3:2 (or 60/40) on cycling between increasing concentration of C_2H_5OH vapor, LPG and NH_3 gas (250, 500, 1000, 1500 and 2000 ppm) and ambient air at 350 °C. It can be seen that the resistance values decreased abruptly with the injection of target gases then increased gradually and recovered its initial values after the test gases were released. The electric resistance of the sensor underwent a decreasing and increasing process when the test gases

were injected and released, respectively, which is consistent with the sensing behavior of n-type semiconductor sensor. The gas sensitivity of the sensor increased dramatically from 13 to 48 as the C_2H_5OH concentration increased from 250 to 2000 ppm. The sensor exhibits the largest response to C_2H_5OH in the other gases, less sensitive to LPG and insensitive to NH_3, showing that the sensor has a rather good selectivity to C_2H_5OH compared with other examined gases at 350 °C. Fig.3c shows the relationship between the gas sensor responses and tested gas concentrations at 350 °C for the α-Fe_2O_3: ZnO=3:2 sensor. The gas sensitivity of the sensor increases linearly to the ethanol concentration from 250 to 2000 ppm. The gas sensitivity to 250 ppm C_2H_5OH at 350 °C is 13. In order to reveal the moments of the gas input and gas stop, the enlarged part of data in Fig.3b measured at a C_2H_5OH concentration of 2000 ppm is illustrated in Fig.3d. After the introduction of 2000 ppm C_2H_5OH vapor, the sensitive response occurs immediately and the 90% sensitive response time and 90% recovery time are 30 s and 420 s, respectively. The slow recovery is attributed to the surface poisoning, fluctuations of temperatures in the surrounding atmosphere and humidity related effects [16]. After many cycles between the test gas and clean air, the resistance of the sensor could recover its initial state with very little baseline drift, which indicates that the response and recovery characteristics are almost reproducible. It indicates that this kind of sensor can be used to detect C_2H_5OH at 350 °C.

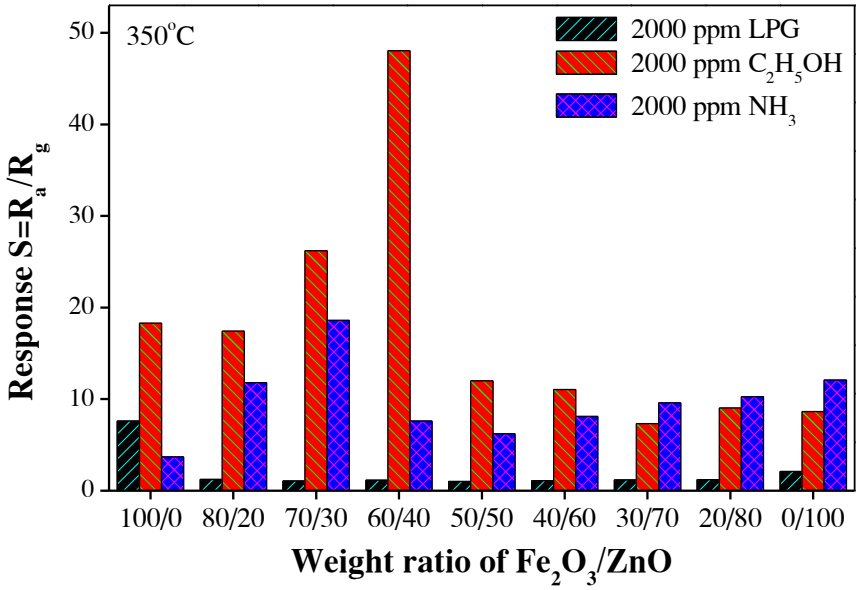

Figure 4. The sensitivity of pristine Fe_2O_3 NRs, bare ZnO NPs and composite sensors with various weight ratios of Fe_2O_3/ZnO to 2000 ppm C_2H_5OH, LPG, NH_3 at 350 °C.

Selectivity is the ability that a gas sensor distinguishes between different kinds of gases. Fig.4 shows the sensitivity of the sensors based on pure ZnO NPs, pure Fe_2O_3 NRs and α-Fe_2O_3/ZnO nanocomposites with different weight ratios to C_2H_5OH, LPG, NH_3 of the same concentration 2000 ppm at operating temperature of 350 °C. The response of the α-Fe_2O_3/ZnO composite (3:2 in weight) to ethanol vapor are about five-fold, four-fold higher than that of other composites (such as 2:3, 4:1). The sensors were also highly selective towards C_2H_5OH which is evident from the selectivity histogram. Sensor based on α-Fe_2O_3/ZnO=3:2 in weight composite exhibited a negligible response towards other interfering gases like LPG and NH_3, while other sensors have poor selectivity. According to the gas sensitivity, response time, it can be concluded that α-Fe_2O_3/ZnO=3:2 is the best composition

comparing to other samples. It was found that response depends upon ZnO content. Compared with pristine α-Fe_2O_3, α-Fe_2O_3/ ZnO composites showed the large response to C_2H_5OH vapor. The reason may be that the partial replacement of Fe^{3+} ions by Zn^{2+} is advantageous to adsorption and oxidation for ethanol gas. The point defect is produced when Zn^{2+} occupied the sites of Fe^{3+} in the crystal and holes will be generated which results in the conductivity of composite samples is considerably lower than that of α-Fe_2O_3. Iron ions are very stable in the +3 valence state, whereas zinc ions tend to stabilize in the +2 valence state, thus influencing the stability of composite structure when Fe and Zn ions exist in trivalent and divalent state, respectively [17].

The gas-sensing mechanism of metal-oxide-semiconductor gas-sensing materials is very complicated which is based on the understanding of chemical reactions between oxygen species and tested gas on metal oxides. The reason for the enhanced C_2H_5OH sensitivity and selectivity of the α-Fe_2O_3/ZnO composite based sensor was put forward. As we know, both ZnO and α-Fe_2O_3 are n-type semiconductive oxides which conduction electrons come from point defects (oxygen vacancies and interstitial metal atoms). Ivanovskaya *et al*. have suggested that ethanol detection is a multi-step process involving both reductive-oxidative and acid-base interaction with a sensor based on heterojunction oxide structures [18]. The change of resistance is mainly caused by the adsorption and desorption of gas molecules on the surface of the sensing structure. In the ambience air, the occurrence of different types of ionosorbed oxygen species on the surface of the material like O_2^-, O^- or O^{2-} is a function of temperature and atmospheric condition. The oxygen species capture electrons from the material, leading a decrease in electron concentration. Electron exchange between oxygen molecules and the oxide surface formed a surface space-charge layer when they are adsorbed at the oxide surface which increases the potential barrier and thus results in a higher resistance [19]. When the sensor is exposed to ethanol, the gas species will react with adsorbed oxygen ions on the material surface to form CO_2 and H_2O and release the trapped electrons back to the conduction band, which leads to an increasing carrier concentration of the sample and results in a decrease the width of the depletion layer, thereby decreasing the sensor resistance according to following reaction:

$$C_2H_5OH + 6O^- \rightarrow 2CO_2 + 3H_2O + 6e^-$$

When the C_2H_5OH concentration is increased, the number of electrons released to the conduction band increases and the barrier in the conduction band of material is further decreased. As a result, the conductivity and the sensitivity are both increased. The gas-sensing behavior of the element is strongly related to its surface which is so-called surface-controlled process. Because of the different band gaps (ZnO: E_g = 3.37 eV, α-Fe_2O_3: E_g = 2.2 eV) [20] and work functions ($\Phi_{ZnO} = 5.2\,eV$, $\Phi_{Fe_2O_3} = 5.88\,eV$) [20], ZnO has a smaller work function compared with α-Fe_2O_3, thus the electrons in the ZnO will migrate to the α-Fe_2O_3 until their Fermi levels equalize which generated an electron depletion layer at the interface between ZnO and Fe_2O_3 that plays an important role in the electron transfer of surface reactions, more trapped electrons are released which results in a thinner space-charge layer and further decreases the potential barrier, so the sensing performance is enhanced (Fig.5).

It is well known that the sensing mechanism of semiconducting oxide gas sensors is based on the surface reaction [21]. The surface-volume ratio of nanocomposite with the composition of Fe_2O_3: ZnO to be 3:2 is highest among other samples, which indicates that the defects increase, resulting in many oxygen vacancies in the materials, so more gas molecules are easy to be adsorbed on the active centers and the sensitivity is increased.

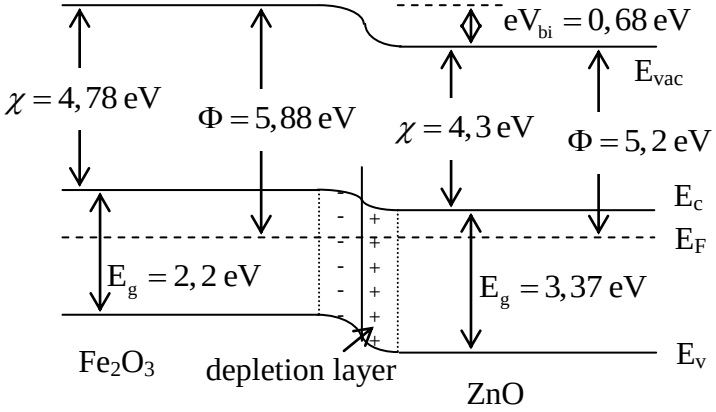

Figure 5. Energy band structure of α-Fe_2O_3/ZnO nanocomposites.

Meanwhile, addition more amount of ZnO NPs may cover the active centers of Fe_2O_3 resulting in decreasing the sensitivity. Limei Huang and Huiqing Fan found that the ZnO nanosheets/α-Fe_2O_3 nanoparticles composites based sensor exhibited a much higher sensitivity to ethanol vapor than the sensor based on pure ZnO nanostructures and the 2% α-Fe_2O_3-added ZnO sensor showed the highest sensitivity [9]. The gas response to ethanol vapor is significantly higher than that to the other gases tested such as toluene, methanol, ammonia, formaldehyde, cyclohexane and methane with a magnitude about 3-27 times greater than that for all the other tested gases under the same concentration. Jun Zhang and co-workers showed that the α-Fe_2O_3/ZnO core-shell nanostructure exhibited more than two times higher sensitivity to ethanol compared with that of pristine α-Fe_2O_3 and exhibited the highest sensitivity to ethanol among all the test gases including acetone, methanol, ether and carbon monoxide [20].

4. Conclusion

In summary, C_2H_5OH sensor based on α-Fe_2O_3/ZnO composite synthesized by hydrothermal technique and soft chemical process have been demonstrated. Blending α-Fe_2O_3 NRs and ZnO NPs resulted in an enhanced response towards C_2H_5OH compared with those of the component α-Fe_2O_3 NRs and ZnO NPs sensors. Sample containing 60 wt.% α-Fe_2O_3 exhibited a sensor response of 48 towards 2000 ppm C_2H_5OH at an operating temperature of 350 °C. This sensor could operate with good sensitivity, selectivity, reproducibility and fast response time, all conditions necessary for practical application. A possible mechanism for the C_2H_5OH-sensing property of the α-Fe_2O_3/ZnO sensor is explored. The enhanced response and the high selectivity are attributed to the formation of random nano n-n hetero-junction between α-Fe_2O_3 nanorods and ZnO nanoparticles, which associated with an enhanced electrostatic barrier at the hetero-junction interface. This composite would be applied to the development of a ethanol vapor detecting micro-sensor system.

Acknowledgements

We would like to thank the support of the Vietnam National Foundation for Science and Technology Development (NAFOSTED) under grant number of 103.02.2015.18.

References

1. Xiaoping Shen, Guoxiu Wang, David Wexler, Large-scale synthesis and gas sensing application of vertically aligned and double-sided tungsten oxide nanorod arrays, Sensors and Actuators B 143 (2009) 325.
2. Yanghai Gui, Fanghong Dong, Yonghui Zhang, Yong Zhang, Junfeng Tian, Preparation and gas sensitivity of WO_3 hollow microspheres and SnO_2 doped heterojunction sensors, Materials Science in Semiconductor Processing 16 (2013) 1531.
3. Dang Duc Vuong, Go Sakai, Kengo Shimanoe, Noboru Yamazoe, Hydrogen sulfide gas sensing properties of thin films derived from SnO_2 sols different in grain size, Sensors and Actuators B 105 (2005) 437.
4. Dang Duc Vuong, Go Sakai, Kengo Shimanoe, Noboru Yamazoe, Preparation of grain size-controlled tin oxide sols by hydrothermal treatment for thin film sensor application, Sensors and Actuators B 103 (2004) 386.
5. Wu Ya-Qiao, Hu Ming, Wei Xiao-Ying, A study of transition from n- to p-type based on hexagonal WO_3 nanorods sensor, Chinese Physics B 23 (2014) 040704.
6. Kengo Shimanoe, Aya Nishiyama, Masayoshi Yuasa, Tetsuya Kida, Noboru Yamazoe, Microstructure control of WO_3 film by adding nano-particles of SnO_2 for NO_2 detection in ppb level, Procedia Chemistry 1 (2009) 212.
7. Yan Wang, Jianliang Cao, Shurong Wang, Xianzhi Guo, Jun Zhang, Huijuan Xia, Shoumin Zhang, Shihua Wu, Facile synthesis of porous α-Fe_2O_3 nanorods and their application in ethanol sensors, Journal of Physical Chemistry C 112 (2008) 17804.
8. Wei-Wei Wang, SnO_2/α-Fe_2O_3 hierarchical nanostructure: Hydrothermal preparation and formation mechanism, Materials Research Bulletin 43 (2008) 2055.
9. Limei Huang, Huiqing Fan, Room-temperature solid state synthesis of ZnO/α-Fe_2O_3 hierarchical nanostructures and their enhanced gas-sensing properties, Sensors and Actuators B 171-172 (2012) 1257.
10. D.R. Patil, L.A. Patil, Preparation and study of NH_3 gas sensing behavior of Fe_2O_3 doped ZnO thick film resistors, Sensors and Transducers Journal 70 (2006) 661.
11. Monica Sorescu, L. Diamandescu, D. Tarabasanu-Mihaila, V.S. Teodorescu, B.H. Howard, Hydrothermal synthesis and structural characterization of $(1-x)\alpha$-Fe_2O_3–$xSnO_2$ nanoparticles, Journal of Physics and Chemistry of Solids 65 (2004) 1021.
12. Dang Duc Vuong, Khuc Quang Trung, Nguyen Hoang Hung, Nguyen Van Hieu, Nguyen Duc Chien, Facile preparation of large-scale α-Fe_2O_3 nanorods/SnO_2 nanorods composites and their LPG-sensing properties, Journal of Alloys and Compounds 599 (2014) 195.
13. Huixiang Tang, Mi Yan, Hui Zhang, Shenzhong Li, Xingfa Ma, Mang Wang, Deren Yang, A selective NH_3 gas sensor based on Fe_2O_3-ZnO nanocomposites at room temperature, Sensors and Actuators B 114 (2006) 910.
14. Suiyuan Chen, Yikun Zhang, Weili Han, Daniel Wellburn, Jing Liang, Changsheng Liu, Synthesis and magnetic properties of Fe_2O_3-TiO_2 nano-composite particles using pulsed laser gas phase evaporation-liquid phase collecting method, Applied Surface Science 283 (2013) 422.
15. Silviya Todorova, Jian-Liang Cao, Daniel Paneva, Krasimir Tenchev, Ivan Mitov, Georgi Kadinov, Zhong-Yong Yuan, Vasko Idakiev, Mesoporous CuO-Fe_2O_3 composite catalysts for complete n-hexane oxidation, Studies in Surface Science and Catalyst 175 (2010) 547.

16. G. Korotcenkov, B.K. Cho, Instability of metal oxide-based conductometric gas sensors and approaches to stability improvement, Sensors and Actuators B 156 (2011) 527.
17. G.N. Chaudhari, S.V. Jagtap, N.N. Gedam, M.J. Pawar, V.S. Sangawar, Sol-gel synthesized semiconducting $LaCo_{0.8}Fe_{0.2}O_3$-based powder for thick film NH_3 gas sensor, Talanta 78 (2009) 1136.
18. M. Ivanovskaya, D. Kotsikau, G. Faglia, P. Nelli, S. Irkaev, Gas-sensitive properties of thin film heterojunction structures based on Fe_2O_3-In_2O_3 nanocomposites, Sensors and Actuators B 93 (2003) 422.
19. Shengyue Wang, Wei Wang, Wenzhong Wang, Zheng Jiao, Jinhuai Liu, Yitai Qian, Characterization and gas-sensing properties of nanocrystalline iron (III) oxide films prepared by ultrasonic spray pyrolysis on silicon, Sensors and Actuators B 69 (2000) 22.
20. Jun Zhang, Xianghong Liu, Liwei Wang, Taili Yang, Xianzhi Guo, Shihua Wu, Shurong Wang, Shoumin Zhang, Synthesis and gas sensing properties of a-Fe_2O_3@ZnO core-shell nanospindles, Nanotechnology 22 (2011) 185501.
21. J. Watson, The tin oxide gas sensor and its applications, Sensors and Actuators 5 (1984) 29.